

# The *Candida albicans* Sur7 Protein Is Needed for Proper Synthesis of the Fibrillar Component of the Cell Wall That Confers Strength<sup>∇</sup>

Hong X. Wang,<sup>1</sup> Lois M. Douglas,<sup>1</sup> Vishukumar Aimanianda,<sup>2</sup>  
Jean-Paul Latgé,<sup>2</sup> and James B. Konopka<sup>1\*</sup>

Department of Molecular Genetics and Microbiology, Stony Brook University, Stony Brook, NY 11794-5222,<sup>1</sup>  
and Unité des Aspergillus, Institut Pasteur, 25 rue du Docteur Roux, 75724 Paris Cedex 15, France<sup>2</sup>

Received 7 July 2010/Accepted 16 November 2010

The *Candida albicans* plasma membrane plays important roles in interfacing with the environment, morphogenesis, and cell wall synthesis. The role of the Sur7 protein in cell wall structure and function was analyzed, since previous studies showed that this plasma membrane protein is needed to prevent abnormal intracellular growth of the cell wall. Sur7 localizes to stable patches in the plasma membrane, known as MCC (membrane compartment occupied by Can1), that are associated with eisosome proteins. The *sur7Δ* mutant cells displayed increased sensitivity to factors that exacerbate cell wall defects, such as detergent (SDS) and the chitin-binding agents calcofluor white and Congo red. The *sur7Δ* cells were also slightly more sensitive to inhibitors that block the synthesis of cell wall chitin (nikkomycin Z) and  $\beta$ -1,3-glucan (caspofungin). In contrast, Fmp45, a paralog of Sur7 that also localizes to punctate plasma membrane patches, did not have a detectable role in cell wall synthesis. Chemical analysis of cell wall composition demonstrated that *sur7Δ* cells contain decreased levels of  $\beta$ -glucan, a glucose polymer that confers rigidity on the cell wall. Consistent with this, *sur7Δ* cells were more sensitive to lysis, which could be partially rescued by increasing the osmolarity of the medium. Interestingly, Sur7 is present in static patches, whereas  $\beta$ -1,3-glucan synthase is mobile in the plasma membrane and is often associated with actin patches. Thus, Sur7 may influence  $\beta$ -glucan synthesis indirectly, perhaps by altering the functions of the cell signaling components that localize to the MCC and eisosome domains.

*Candida albicans* is the most common human fungal pathogen. Although it is a commensal organism of humans, under certain conditions it causes life-threatening infections in susceptible individuals (18, 27). One feature that underlies the pathogenesis of *C. albicans* is its ability to grow in different morphologies, including buds, elongated pseudohyphae, and long filamentous hyphal cells (35). Induction of the hyphal form correlates with increased expression of virulence factors, including adhesin proteins that promote biofilm formation and attachment to human cells, secreted hydrolytic enzymes that facilitate invasive growth and inactivate components of the complement pathway, and antioxidant enzymes that counteract the immune system (5, 7, 20, 40). The role of the plasma membrane has been under investigation in *C. albicans* pathogenesis because of the critical roles that it plays in the production of virulence factors and in transducing information and nutrients from the extracellular environment. The plasma membrane is also involved in dynamic cellular processes, such as secretion, endocytosis, and cell wall biogenesis, that are essential for proper morphogenesis and viability. The critical role of the plasma membrane is highlighted by the fact that it is the target of the most commonly used antifungal drugs (28).

The *Saccharomyces cerevisiae* plasma membrane is composed of at least two different subdomains (24, 25). One do-

main, termed MCP (membrane compartment occupied by Pma1), contains proteins that readily diffuse, such as the plasma membrane ATPase Pma1. Another domain appears as 300-nm patches that are immobile in the membrane. The latter domain was termed MCC (membrane compartment occupied by Can1), since it contains the Can1 arginine permease (24, 25). These static MCC domains are distinct from the mobile cortical actin patches or the finger-like invaginations that form at sites of endocytosis. Subsequent studies identified other symporters in the MCC and also two families of proteins that are thought to contain four transmembrane domains (TMDs) (15, 17). The best-known examples of these two different families of tetra-spanning proteins are Nce102 and Sur7. Nce102 has been implicated in sphingolipid signaling that regulates the formation of the MCC domains (15). The function of Sur7 in *S. cerevisiae* is not clear, perhaps because of genetic redundancy, since there are at least three paralogs of Sur7 (Fmp45, Ylr414c, and Pun1/Ynl194c) (2, 44). Mutation of the *SUR7* family members does not cause strong phenotypes under standard growth conditions (2, 44), although Pun1 was recently shown to be important for proper response to nitrogen stress (43). Pun1/Ynl194c is more divergent than the other members of the Sur7 family in *S. cerevisiae*, including differences in the Cys-containing motif in extracellular loop 1 of Sur7 family proteins and at the analogous position in the mammalian Claudin proteins found at tight junctions (2). In contrast, *C. albicans* contains just two members of this family, Sur7 and Fmp45. This suggests that the functions of Sur7 family members may have diverged between *S. cerevisiae* and *C. albicans*.

The structure of the MCC domains was broadened by iden-

\* Corresponding author. Mailing address: Department of Molecular Genetics and Microbiology, Stony Brook University, Stony Brook, NY 11794-5222. Phone: (631) 632-8715. Fax: (631) 632-9797. E-mail: jkonopka@ms.cc.sunysb.edu.

<sup>∇</sup> Published ahead of print on 29 November 2010.

TABLE 1. Strains used in this study

<i>C. albicans</i> strain	Parent	Genotype
BWP17	Sc5314	<i>ura3Δ::nim434/ura3Δ::nim434 his1::hisG/his1::hisG arg4::hisG/arg4::hisG</i>
DIC185	BWP17	<i>ura3Δ::nim434/URA3 his1::hisG/HIS1 arg4::hisG/ARG4</i>
YJA10	BWP17	<i>sur7Δ::ARG4/sur7Δ::HIS1 ura3Δ::nim434/ura3Δ::nim434 his1::hisG/his1::hisG arg4::hisG/arg4::hisG</i>
YJA11	YJA10	<i>sur7Δ::ARG4/sur7Δ::HIS1 URA3/ura3Δ::nim434 his1::hisG/his1::hisG arg4::hisG/arg4::hisG</i>
YJA12	YJA10	<i>sur7Δ::ARG4/sur7Δ::HIS1 SUR7::URA3 ura3Δ::nim434/ura3Δ::nim434 his1::hisG/his1::hisG arg4::hisG/arg4::hisG</i>
YHXW1	BWP17	<i>fmp45Δ::ARG4/FMP45 ura3Δ::nim434/ura3Δ::nim434 his1::hisG/his1::hisG arg4::hisG/arg4::hisG</i>
YHXW2	YHXW1	<i>fmp45Δ::ARG4/fmp45Δ::HIS1 ura3Δ::nim434/ura3Δ::nim434 his1::hisG/his1::hisG arg4::hisG/arg4::hisG</i>
YHXW3	YHXW2	<i>fmp45Δ::ARG4/fmp45Δ::HIS1 URA3/ura3Δ::nim434 his1::hisG/his1::hisG arg4::hisG/arg4::hisG</i>
YHXW4	BWP17	BWP17, except <i>SUR7-GFPγ::URA3</i>
YHXW5	BWP17	BWP17, except <i>FMP45-GFPγ::URA3</i>
YHXW6	YJA10	<i>sur7Δ</i> strain YJA10, except <i>FMP45-GFPγ::URA3</i>
YHXW7	YHXW2	<i>fmp45Δ</i> strain YHXW2, except <i>SUR7-GFPγ::URA3</i>
YHXW8	YHXW2	<i>fmp45Δ::NAT/fmp45Δ::HIS1 ura3Δ::nim434/ura3Δ::nim434 his1::hisG/his1::hisG arg4::hisG/arg4::hisG</i>
YHXW9	YHXW8	<i>fmp45Δ::NAT/fmp45Δ::HIS1 sur7Δ::UAU/SUR7 ura3Δ::nim434/ura3Δ::nim434 his1::hisG/his1::hisG arg4::hisG/arg4::hisG</i>
YHXW10-UAU1	YHXW9	<i>fmp45Δ::NAT/fmp45Δ::HIS1 sur7Δ::UAU/sur7Δ::URA3 ura3Δ::nim434/ura3Δ::nim434 his1::hisG/his1::hisG arg4::hisG/arg4::hisG</i>
YHXW10-UAU2	YHXW9	<i>fmp45Δ::NAT/fmp45Δ::HIS1 sur7Δ::UAU/sur7Δ::URA3 ura3Δ::nim434/ura3Δ::nim434 his1::hisG/his1::hisG arg4::hisG/arg4::hisG</i>
YHXW10-UAU3	YHXW9	<i>fmp45Δ::NAT/fmp45Δ::HIS1 sur7Δ::UAU/sur7Δ::URA3 ura3Δ::nim434/ura3Δ::nim434 his1::hisG/his1::hisG arg4::hisG/arg4::hisG</i>

tification of a complex of cytoplasmic proteins known as eisosomes that associate with the inner surface of the plasma membrane at MCC sites (39). Eisosomes have been implicated in endocytosis, but it is not clear how these static domains relate to sites of endocytosis mediated by actin patches, since these regions appear to be distinct in the plasma membrane (39, 44). However, there is likely to be at least an indirect link. Two proteins that localize to eisosomes, Pil1 and Lsp1, are needed for proper rates of endocytosis (39). Pil1 and Lsp1 associate with the Pkh1/2 protein kinases (23, 38) that influence endocytosis and a variety of other processes, including cell wall integrity, actin localization, and response to heat stress (10, 23). Pkh1/2 also mediate the effects of sphingolipids on the regulation of the assembly and disassembly of eisosomes by phosphorylating Pil1 and Lsp1 (23, 38).

Analysis of a *C. albicans sur7Δ* (*Casur7Δ*) mutant implicated the MCC domains in the regulation of cell wall synthesis. In contrast to *S. cerevisiae*, a *Casur7Δ* mutant displayed obvious defects in bud and hyphal morphogenesis (1–3). Interestingly, the mutant cells showed an unusual phenotype in that there were large intracellular regions of cell wall growth. The abnormal cell wall synthesis was suggested to be due in part to a defect in  $\beta$ -1,3-glucan synthesis, since the *sur7Δ* mutant showed changes in gene expression that overlapped with those observed when cells are treated with caspofungin, an inhibitor of cell wall  $\beta$ -1,3-glucan synthase (2). In addition, septins were mislocalized in *sur7Δ* cells, analogous to the altered localization of septins caused by treatment of cells with caspofungin (4). Therefore, *C. albicans sur7Δ* and *fmp45Δ* mutants were analyzed in this study to determine how the structure and function of the cell wall were altered. The results demonstrated that Sur7 is important for resistance to conditions that perturb cell wall function and also for the proper synthesis of the  $\beta$ -1,3-glucan component of the cell wall.

## MATERIALS AND METHODS

**Strains and media.** The *C. albicans* strains (Table 1) were propagated on rich YPD medium (2% glucose, 1% peptone, and 2% yeast extract) or on SD (yeast nitrogen base synthetic medium with dextrose), essentially as described previously (34). Uridine (80 mg/liter) was added to cultures of *ura3Δ* cells. Hyphal morphogenesis was monitored by growing cells at 37°C in medium containing 10% bovine calf serum. Invasive growth was assayed by spotting  $3 \times 10^3$  cells onto agar medium containing 4% bovine calf serum and then incubating the plates for 7 days at 37°C.

The *C. albicans sur7Δ* homozygous deletion mutant and the *sur7Δ*- plus *SUR7*-complemented strain were constructed previously in *C. albicans* strain BWP17 (2). The *fmp45Δ* homozygous deletion mutant was constructed using similar methods. In brief, PCR primers that contained ~70 bp of sequence homologous to the 5' and 3' ends of the *FMP45* open reading frame were used to amplify a cassette containing either the *ARG4* or the *HIS1* selectable marker gene (41). The *sur7Δ fmp45Δ* double mutants were constructed using the UAU method (13). The starting strain for this procedure was YHXW8 (*fmp45::HIS1 fmp45::NAT*), which was constructed in part by using the SAT-flipper (32). One allele of *SUR7* was then deleted by homologous recombination with the UAU cassette and identified after selection on medium lacking arginine. The UAU cassette consists of an *ARG4* gene flanked by the 5' and 3' portions of the *URA3* gene (13). The mutant cells were then grown nonselectively to permit the endogenous recombination pathways to replace the other allele of *SUR7* to generate a *sur7::UAU/sur7::UAU* homozygous deletion. Segregants were then isolated on medium lacking Arg and Ura to identify cells that underwent a further recombination event that converts one UAU allele into a functional *URA3* gene by looping out the *ARG4* sequences. More than 30% of the Arg<sup>+</sup> Ura<sup>+</sup> colonies contained a homozygous deletion, *sur7::UAU/sur7::URA3*, and lacked the wild-type *SUR7* gene, which is similar to the frequency reported for other nonessential genes (13). Integration of the deletion cassettes at the appropriate sites was verified by PCR using combinations of primers that flanked the integration site and also primers that annealed within the introduced cassettes.

The 3' ends of the *SUR7* and *FMP45* open reading frames were fused to green fluorescent protein (GFP) via homologous recombination using previously described methods (45). PCR primers containing ~70 bp of sequence homologous to the 3' end of the *SUR7* or *FMP45* open reading frames were used to amplify a cassette containing a more photostable version of enhanced GFP (CaGFP $\gamma$ ) and a *URA3* selectable marker (45). The Ura<sup>+</sup> colonies resulting from the transformation of the cassette into *C. albicans* were then screened for GFP-positive cells by fluorescence microscopy and confirmed by PCR.

**Microscopy.** Cells used for microscopic analysis of Sur7-GFP and Fmp45-GFP were grown overnight to log phase. Fluorescence microscopy was used to detect GFP, and differential interference contrast (DIC) optics was used to detect cell morphology. Chitin staining was carried out by incubating cells with 40 ng/ml calcofluor white (Sigma-Aldrich) as described previously (29). In order to visualize the intracellular growth of the cell wall, cells were first permeabilized by washing them with methanol and acetone and then stained with calcofluor white. Covalent labeling of the cell walls with the fluorescent dye fluorescein was carried out by washing the cells 3 times in phosphate-buffered saline (PBS), resuspending them at  $10^8$  cells/ml in PBS, and then adding fluorescein-5-maleimide (FM) (Invitrogen) to a final concentration of 0.2  $\mu\text{g/ml}$ . The cells were incubated for 15 min, washed 3 times with PBS, and then resuspended in YPD medium. Labeling the cells with FM in this manner did not have detectable effects on growth. At different times after FM labeling, the cells were permeabilized as described above and then stained with 4  $\mu\text{g/ml}$  calcofluor white. Cell integrity was analyzed by mixing equal volumes of cell culture and a solution of 0.4% trypan blue (Sigma-Aldrich), incubating them for 5 min, and then visualizing them by light microscopy to identify lysed cells that stained blue. Images were captured using an Olympus BH2 microscope equipped with a Zeiss Axio-Cam digital camera.

**Drug and chemical sensitivity.** Sensitivity to SDS, Congo red, calcofluor white, and hygromycin was tested by spotting dilutions of cells onto YPD plates prepared with the indicated concentration of the corresponding chemical. Three microliters of a 10-fold dilution series of cells was spotted on the surfaces of the plates. The plates were then incubated at 37°C for the indicated time and photographed. The sensitivity of cells to nikkomycin Z, rapamycin, and tunicamycin was assayed by testing the effects of a serial dilution series of drug concentrations in 96-well plates. The cells were adjusted to  $1 \times 10^4$  cells/ml in SD medium and plated in the wells, and then a 2-fold dilution series of the indicated drug was applied. The plates were incubated at 37°C for 2 days, and the extent of growth was quantified with a spectrophotometer. Sensitivities to fluconazole, amphotericin, and caspofungin were assayed using Etest strips according to the manufacturer's directions (bioMérieux, Inc., Durham, NC). In brief,  $1 \times 10^6$  cells were spread on an agar plate containing RPMI 1640 medium (Sigma-Aldrich), 0.165 M MOPS (morpholinepropanesulfonic acid), pH 7, and 2% dextrose; an Etest strip was applied; and the plates were incubated at 37°C for 48 h.

**Chemical analysis of cell wall composition.** Strains were adjusted to an optical density at 600 nm ( $\text{OD}_{600}$ ) of 0.01 and then grown in YPD at 30°C for 15 h. The cells were washed twice with water and boiled twice in 50 mM Tris-HCl buffer (pH 7.5) containing 50 mM EDTA, 2% SDS, and 40 mM  $\beta$ -mercaptoethanol for 1 h. The sediment obtained after centrifugation (3,600 rpm; 10 min) was washed five times with water and then incubated twice in 1 M NaOH containing 0.5 M  $\text{NaBH}_4$  at 65°C for 1 h. The insoluble pellet obtained upon centrifugation (3,600 rpm; 10 min) was washed with water to neutrality and freeze-dried (alkali-insoluble [AI] fraction). The supernatant fraction was then neutralized, dialyzed against water, and freeze-dried (alkali-soluble [AS] fraction). The monosaccharide composition was determined by gas-liquid chromatography (GLC) (Perichrom PR2100 instrument; Perichrom, Saulx-les-Chartreux, France) equipped with a flame ionization detector (FID) and a fused silica capillary column (30 m by 0.32-mm inside diameter; filled with BP1 matrix composed of dimethyl polysiloxane) using mesoinositol as the internal standard. Derivatized hexoses (alditol acetates) were obtained after hydrolysis (4 N trifluoroacetic acid/8 N hydrochloric acid; 100°C for 4 h) of the AI and AS fractions, followed by reduction and peracetylation. The monosaccharide composition (percent) was calculated from the peak areas with respect to that of the internal standard (14).

## RESULTS

**Sur7-GFP and Fmp45-GFP localize to punctate plasma membrane domains in *C. albicans*.** Analysis of the *C. albicans* genome detected only one paralog of Sur7, named Fmp45, which showed 37% identity and 54% similarity to the Sur7 sequence. In contrast, *S. cerevisiae* contains at least three paralogs of Sur7 (Fmp45, Ylr414c, and Pun1/Ynl194c). Although the *C. albicans* paralog of Sur7 was previously named Fmp45, it shows approximately equal amino acid sequence relatedness to *S. cerevisiae* Fmp45 and Ynl194c (31% identity). To determine if CaFmp45 was present in punctate patches in the plasma membrane, we examined the localization of proteins that were fused to GFP. For this analysis, a recently described

version of GFP (GFP $\gamma$ ) that is more photostable (45) was fused to the C-terminal coding sequences of *SUR7* and *FMP45*. As expected, Sur7-GFP was detected in a punctate pattern in the plasma membrane in mother cells but was only weakly detected in new buds (Fig. 1A). Fmp45-GFP was also detected in punctate structures in mother cells, in agreement with previous reports for Fmp45-GFP in *S. cerevisiae* and *C. albicans* (3, 44). In contrast to Sur7-GFP, however, we also detected Fmp45-GFP in new buds. The Fmp45-GFP present in small buds was distributed in a more homogeneous fashion and was not concentrated into punctate domains as it was in mature cells (Fig. 1A). Thus, Sur7-GFP and Fmp45-GFP give similar, but not identical, localization patterns.

**Analysis of cell wall localization in *sur7* $\Delta$  and *fmp45* $\Delta$  cells.** To determine whether Fmp45 functions in cell wall morphogenesis, a homozygous *fmp45* $\Delta$  deletion mutant was constructed in the *C. albicans* BWP17 strain. Microscopic analysis of live cells did not reveal obvious morphological defects for the *fmp45* $\Delta$  cells; they formed buds (Fig. 2A) and hyphae (data not shown) that were similar to those of the wild-type control strain. The *fmp45* $\Delta$  cells also did not contain the intracellular growth of the cell wall seen in the *sur7* $\Delta$  mutant (Fig. 2A, bottom), and Sur7-GFP localized properly in the *fmp45* $\Delta$  cells (Fig. 1B). The *fmp45* $\Delta$  mutant also was not defective in invasive growth into agar, as was the *sur7* $\Delta$  mutant (Fig. 2B). In contrast, as reported previously (2), about half the *sur7* $\Delta$  mutant cells showed obvious morphological defects, including enlarged cells and bud necks, and many cells displayed ectopic intracellular growth of the cell wall (Fig. 2A). Fmp45-GFP was detected at greatly reduced levels in *sur7* $\Delta$  cells, demonstrating that Sur7 is required for normal organization of MCC domains (Fig. 1B).

Older cells were examined to search more sensitively for a weak phenotype caused by *fmp45* $\Delta$ . The rationale for this was based on a previous suggestion that older *sur7* $\Delta$  mutant cells may have more severe defects than younger cells, since most of the new buds appeared to be relatively normal (2). To identify older cells in the population, the cells were covalently labeled with FM so that they could be detected by fluorescence microscopy, whereas any new cells that formed subsequent to the labeling procedure would not be fluorescent. The FM-labeled cells were then grown for 6 h at 30°C, permeabilized, and analyzed by staining the cell wall with calcofluor white. The older FM-labeled *fmp45* $\Delta$  cells did not show any obvious differences from the wild-type control strain (Fig. 2C). In contrast, nearly all of the older *sur7* $\Delta$  mutant cells showed altered calcofluor white staining of the outer cell wall and intracellular growth of the cell wall (Fig. 2C). Time course studies demonstrated that the percentage of FM-labeled *sur7* $\Delta$  cells with cell wall abnormalities increased over time from ~45% to ~90% at the 6-h time point (Fig. 2D). Interestingly, the newer cells that were not fluorescent developed altered cell wall structures as early as 2 h after FM labeling (Fig. 2C and D). The altered cell wall localization in the newer (non-FM-labeled) cells increased over time to a steady-state level of about 45% by 6 h. Thus, the *sur7* $\Delta$  mutant accumulates cell wall abnormalities over time, indicating defects in both the spatial and temporal regulation of wall synthesis.

**The *sur7* $\Delta$  mutant is more sensitive to agents that exacerbate cell wall defects.** The *sur7* $\Delta$  mutant forms extra ectopic



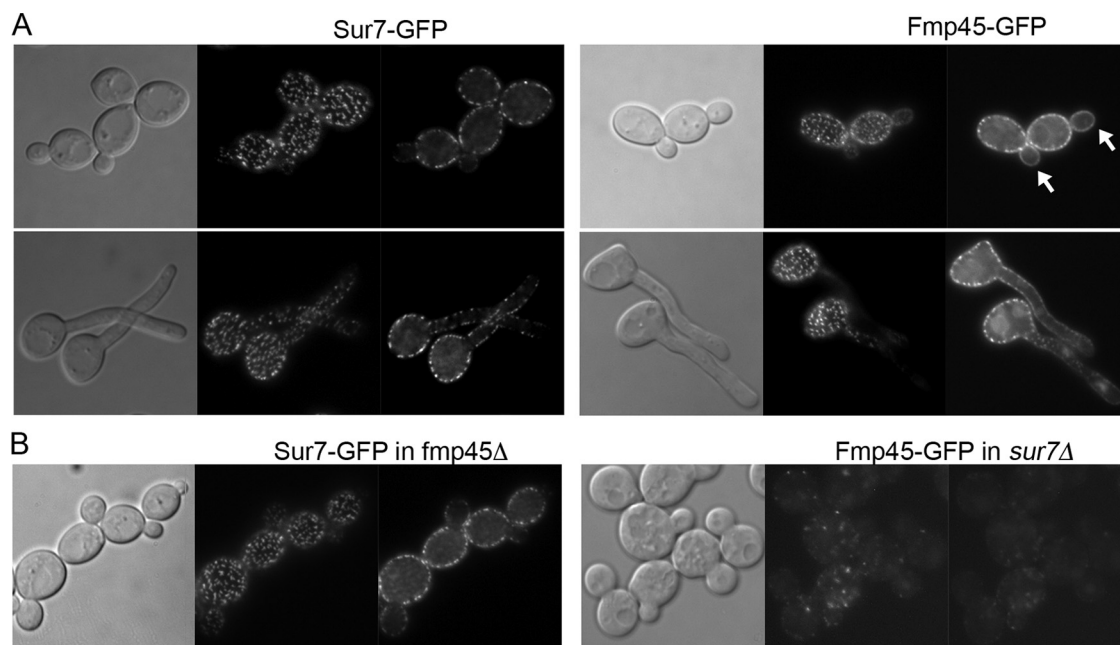


FIG. 1. Punctate plasma membrane localization of Sur7-GFP and Fmp45-GFP. (A) *C. albicans* strain BWP17 engineered to express *SUR7-GFP* or *FMP45-GFP* fusion genes. (Top) Budding cells. (Bottom) Cells induced with 10% bovine calf serum to form hyphae. In each series of images, the image on the left is a light microscope image to show cell morphology. The two fluorescence microscope images on the right demonstrate the localization of Sur7-GFP and Fmp45-GFP in punctate patches in focal planes that correspond to the top of the cell and to the medial portion. The arrows indicate bud localization of Fmp45-GFP. (B) Localization of Sur7-GFP in *fmp45Δ* cells and Fmp45-GFP in *sur7Δ* cells. The microscope images are as described for panel A. All of the fusion genes were constructed with GFP $\gamma$ , a more photostable version of GFP (45). The strains used in these experiments included YHXW4 (*SUR7-GFP*), YHXW5 (*FMP45-GFP*), YHXW6 (*sur7Δ FMP45-GFP*), and YHXW7 (*fmp45Δ SUR7-GFP*).

cell wall, but it is not clear whether this affects the function of the cell wall. To investigate this, the *sur7Δ* and *fmp45Δ* mutants were analyzed for the ability to grow on agar medium containing compounds that exacerbate the growth defects of cell wall synthesis mutants, including SDS, calcofluor white, Congo red, and hygromycin (9). Interestingly, the *sur7Δ* mutant showed greatly increased sensitivity to all four of these reagents, whereas the *fmp45Δ* mutant did not (Fig. 3). Calcofluor white and Congo red are thought to perturb cell wall synthesis by binding to the chitin component of the cell wall. The basis for the sensitivity to SDS is not known, but it may be due to enhanced sensitivity of cell wall synthesis components or a general effect on the plasma membrane. Hygromycin is an aminoglycoside antibiotic whose ability to inhibit protein synthesis is increased in a wide range of cell wall mutants for unknown reasons. Altogether, these results indicate that the *sur7Δ* mutant forms defective cell walls.

**Sensitivity to antifungal drugs.** The mutant cells were analyzed further by testing their sensitivity to drugs that perturb cell wall synthesis. The Pkc1 cell wall stress pathway is expected to play an important role in cells that form abnormal cell walls. To test this, broth dilution assays in 96-well plates were used to examine sensitivity to the drug cercosporamide, which is a selective inhibitor of the *C. albicans* Pkc1 protein kinase (36). The results demonstrated that *sur7Δ* cells were 8-fold more sensitive, consistent with the mutant cells forming defective cell walls (Fig. 4A). The *sur7Δ* mutant was also about 50% more sensitive to nikkomycin Z, an inhibitor of chitin synthase (Fig. 4A), but showed normal sensitivity to tunicamycin,

an inhibitor of N-linked glycosylation that is expected to perturb a wide range of glycosylated cell wall proteins. As reported previously, Etest assays showed that the *sur7Δ* mutant was 2-fold more sensitive to caspofungin (2). Thus, the *sur7Δ* mutant is slightly more sensitive to inhibitors of both chitin and  $\beta$ -glucan synthases. The *sur7Δ* mutant was not hypersensitive to all compounds that exacerbate the defects of cell wall mutants. For example, it showed only a slight difference in sensitivity to rapamycin ( $\leq 2$ -fold) and was not sensitive to a high calcium concentration (0.5 M) (data not shown).

The *fmp45Δ* mutant did not display increased sensitivity to cercosporamide or inhibitors of cell wall synthesis. Etest strip assays also showed that *fmp45Δ* did not show increased sensitivity to fluconazole (data not shown), as does *sur7Δ* (2). Furthermore, we did not detect increased sensitivity of the *fmp45Δ* homozygous deletion mutant to amphotericin (Fig. 4B), which contrasts with a previous report from a high-throughput study that an *fmp45Δ/FMP45* heterozygote is more sensitive to amphotericin (42).

**Altered cell wall composition of *sur7Δ* cells.** The carbohydrate composition of the *sur7Δ* cell wall was analyzed to determine if the constituents were altered compared to the wild-type control strain. The cell walls were divided into AI and AS fractions (see Materials and Methods). Interestingly, the *sur7Δ* mutant showed a decrease in the AI fraction of the cell wall that includes the important structural polymers, chitin and  $\beta$ -glucan (Fig. 5A). The AI/AS ratio decreased from  $3.2 \pm 0.5$  for the wild-type control (DIC185) to  $1.9 \pm 0.2$  for the *sur7Δ* strain (Fig. 5B). Analysis of the monosaccharide composition

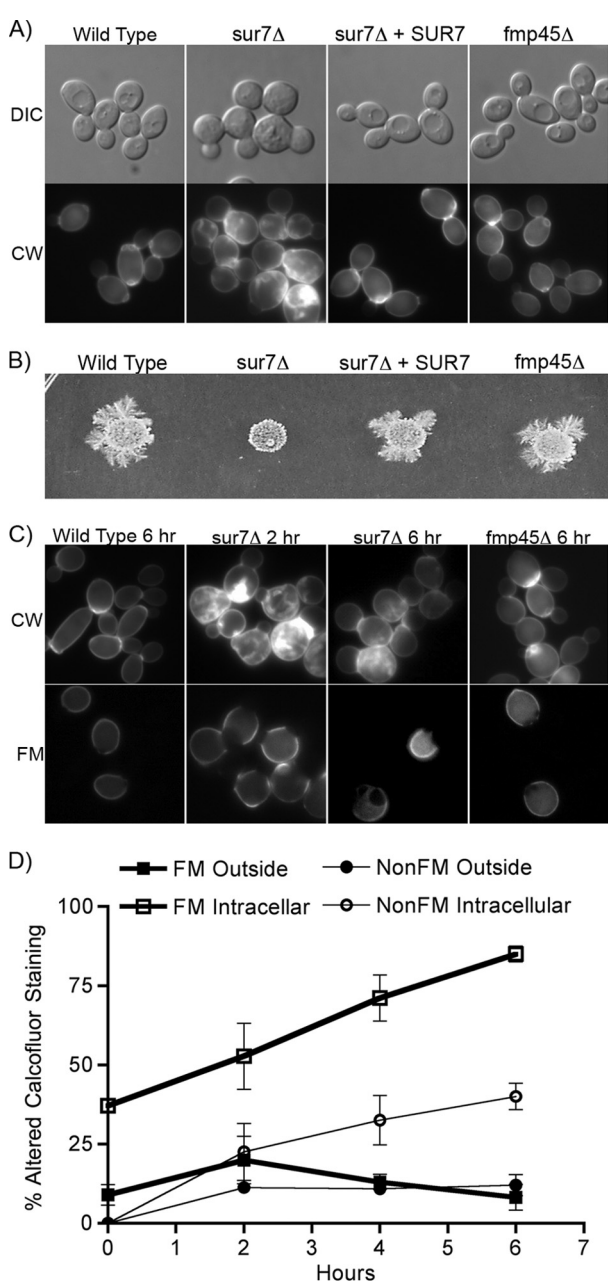


FIG. 2. Analysis of the cell wall and morphogenesis phenotypes of the *sur7Δ* and *fmp45Δ* mutants. (A) The morphology of live cells of the indicated genotypes is shown in the upper images. The lower images show a different set of cells, viewed by fluorescence microscopy, that were permeabilized and stained with calcofluor white to detect cell wall structures. (B) Invasive-growth assay of the indicated *C. albicans* strains. Equal numbers of cells were spotted onto an agar plate containing 4% serum and then incubated at 37°C for 7 days. (C) Comparison of cell wall structures in older and newer cells. Cells of the indicated genotype were cross-linked to fluorescein-maleimide and then grown for 2 or 6 h at 30°C in YPD. The cells were then permeabilized and stained with calcofluor white. Fluorescence microscope images of cells stained with calcofluor white are shown above; the older cells that were cross-linked with fluorescein are shown below. (D) Quantitation of calcofluor white-stained cells after labeling with FM at time zero versus new cells that were not labeled (NonFM). Outside, cells that showed altered calcofluor white staining of the outer cell wall; Intracellular, altered calcofluor white staining within the cell due to ectopic growth of the cell wall. The error bars indicate SD.

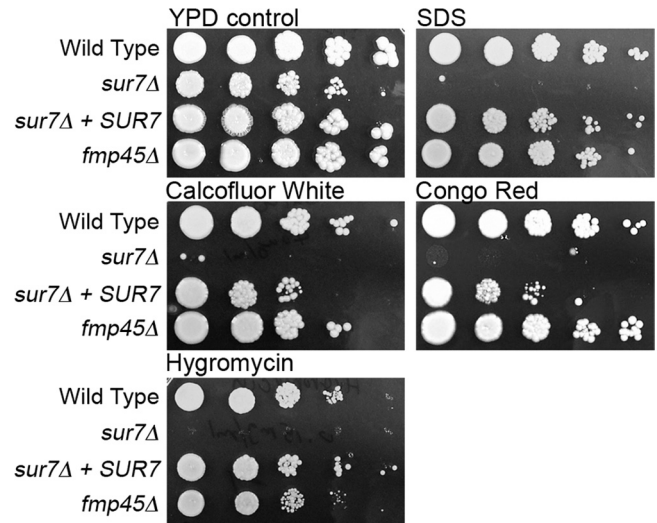


FIG. 3. The *sur7Δ* mutant is more sensitive to chemicals that exacerbate the growth defects of cell wall mutants. Ten-fold dilutions of the wild-type control strain DIC185, YJA11 (*sur7Δ*), YJA12 (*sur7Δ* plus *SUR7*), and YHXW3 (*fmp45Δ*) were spotted onto rich-medium YPD plates containing the following concentrations of the indicated additive: 0.06% SDS, 0.04 mg/ml calcofluor white, 0.1 mg/ml Congo red, and 0.15 mg/ml hygromycin. The plates were incubated at 37°C for 2 days and then photographed.

in the AI fraction from the wild-type control strain DIC185 showed that glucose was the major component, consistent with  $\beta$ -glucan being the most abundant fraction of the cell wall. There was a significant decrease ( $P < 0.01$ ) in the glucose content in the *sur7Δ* cell wall AI fraction compared to that of the wild-type control strain (Fig. 5C). The levels of glucosamine detected in the AI fractions, which correspond to *N*-acetylglucosamine (GlcNAc) in the cell wall, were not significantly different for the wild-type and *sur7Δ* mutant strains (Fig. 5D), even though increased GlcNAc is often detected in cell wall mutants due to a compensatory mechanism that increases chitin levels. In contrast, the AS fraction was increased in the *sur7Δ* cells, mainly due to an elevated mannose content (Fig. 5E). The reduced AI/AS ratio and the low level of  $\beta$ -glucan suggest that the *sur7Δ* cells are likely to form weaker cell walls.

**Osmotic rescue of the *sur7Δ* cell lysis defect.** The altered cell wall composition suggested that *sur7Δ* cells would be more sensitive to lysis. To test this, cells were grown at 42°C, since elevated temperature promotes cell wall stress. As expected, only a small percentage of the cells of the wild-type control strain DIC185 stained with trypan blue, a vital stain used to determine cell viability. In contrast, the *sur7Δ* cells grew more slowly than the wild type at 42°C, and trypan blue staining demonstrated that there was a large fraction of lysed cells. More than 40% of the *sur7Δ* cells stained with trypan blue at 42°C in either rich YPD or synthetic SD medium, indicating that the cells had lysed and the trypan blue dye could gain access to the interior of the cell (Fig. 6). Increasing the osmolarity by adding 1 M sorbitol to the medium decreased the percentage of trypan blue staining from 41.5% to 20.9% in rich medium and 45.7% to 14.9% in synthetic SD medium. Similar results were observed for medium with 1 M NaCl (data not shown). The observation that increased osmolarity decreased

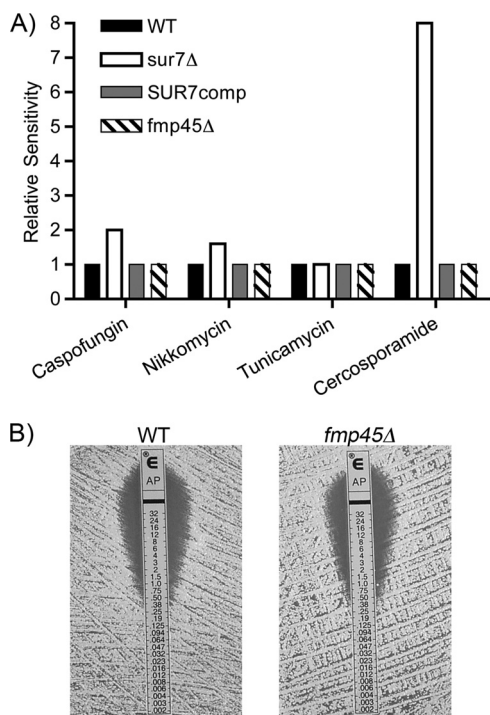


FIG. 4. Altered sensitivity of the *sur7Δ* mutant to antifungal drugs. (A) *C. albicans* strains were tested for sensitivity to nikkomycin Z, tunicamycin, and cercosporamide by assaying their ability to grow in 96-well plates containing a 2-fold dilution series of each drug. Sensitivity to caspofungin was tested with Etest strips, as described previously for the *sur7Δ* mutant (2). The results represent the average of at least two independent experiments. (B) The *fmp45Δ* mutant displays a wild-type level of sensitivity to amphotericin. Cells were spread on a plate containing RPMI 1640 medium, the Etest strip was applied, and then the plates were incubated at 37°C for 48 h. The Etest strips release a gradient of drug, causing a zone of growth inhibition. The strains used in these assays included DIC185, YJA11 (*sur7Δ*), YJA12 (*sur7Δ* plus *SUR7*), and YHXW3 (*fmp45Δ*).

the number of trypan blue-stained *sur7Δ* cells confirms that the lysis defect is due at least in part to weakened cell walls.

Microscopic analysis of the cells also revealed that both large and small *sur7Δ* cells stained with trypan blue. When the *sur7Δ* mutant was grown in rich YPD medium at 30°C, most of the cells that stained with trypan blue were larger. It is not surprising that the larger cells observed in the *sur7Δ* mutant cultures would lyse more readily, since their increased volume places extra demands on the cell wall. However, it was interesting that some smaller cells also stained with trypan blue (Fig. 7A). The lysis of smaller cells was more obvious when the cells were grown in synthetic SD medium, since the *sur7Δ* mutant formed fewer large cells under these conditions but still showed lysis of smaller cells (Fig. 7B). These results indicate that the *sur7Δ* mutation causes defects in cell wall synthesis in younger cells, as well as the older, larger cells that have accumulated more of the aberrant ectopic cell wall structures.

**Deletion of FMP45 does not exacerbate the phenotype of *sur7Δ* cells.** Double-mutant *sur7Δ fmp45Δ* cells were analyzed to determine whether Fmp45 plays a significant role in the absence of Sur7. In view of the possibility that the double mutation may cause lethality, we used the UAU method to

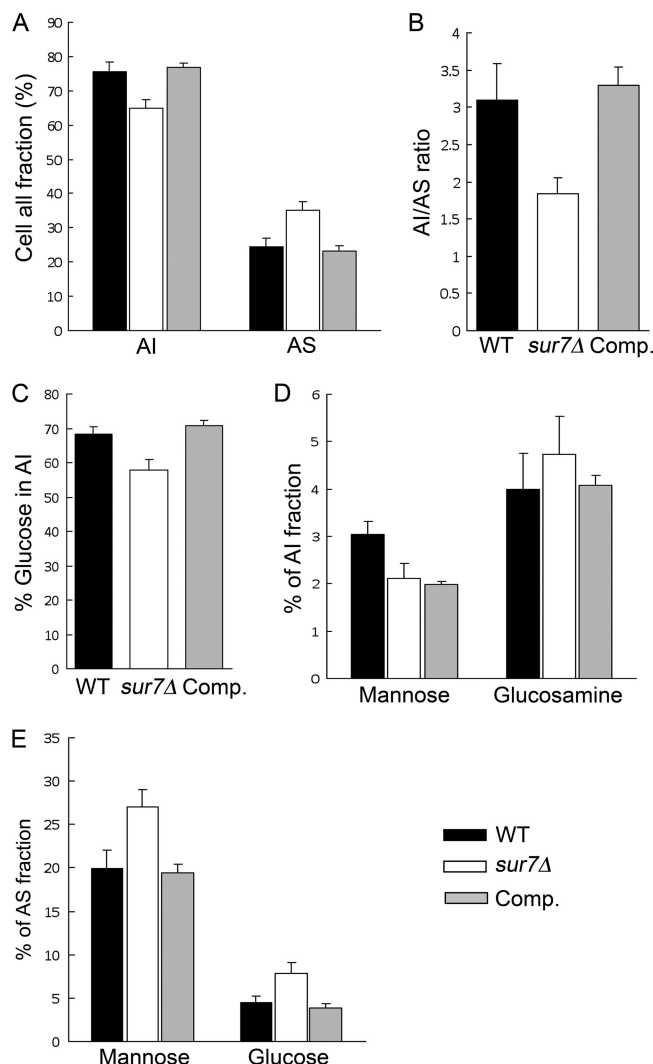


FIG. 5. Decreased alkali-insoluble fraction in *sur7Δ* cell walls. The chemical compositions of the cell walls for the wild-type (DIC185), *sur7Δ* (YJA11), and *sur7Δ* plus *SUR7* complemented (YJA12) strains were compared. (A) Relative amounts of AS and AI fractions as a percentage of the total dry weight of the cell wall. (B) AI/AS ratio for each strain. (C) Glucose compositions of the AI fractions. (D) Mannose and glucosamine compositions of the AI fractions. (E) Mannose and glucose compositions of the AS fractions. Cell wall fractions were analyzed as described in Materials and Methods. The results represent the average of 4 independent experiments plus SD.

create a *sur7Δ fmp45Δ* mutant strain (13). The UAU method entails deleting one copy of a gene with the UAU cassette (an *ARG4* gene flanked by the 5' and 3' portions of a *URA3* gene) and then selecting on medium lacking arginine and uridine for cells in which both copies of the targeted gene are deleted (see Materials and Methods). This approach was successful in yielding *sur7Δ fmp45Δ* mutants, three of which were picked for analysis. The double mutants showed ectopic staining of cell wall chitin (Fig. 8A), increased cercosporamide sensitivity (Fig. 8C), and lysis at 42°C (Fig. 8D) that was similar to that of the *sur7Δ* single mutant, but not worse. The three *sur7Δ fmp45Δ* mutants were also better able to form hyphae in response to serum than *sur7Δ* alone (Fig. 8B), suggesting the possibility



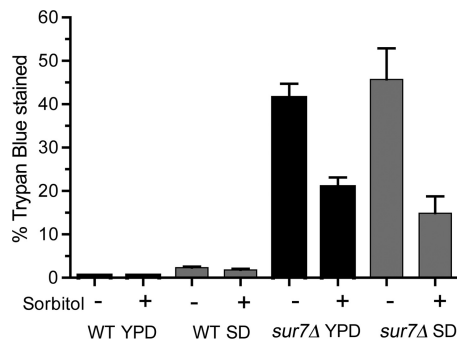


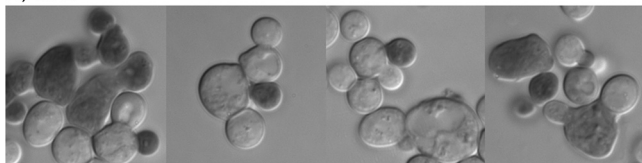
FIG. 6. Increased osmolarity suppresses the cell lysis defect of the *sur7Δ* mutant at elevated temperatures. Wild-type (DIC185) and *sur7Δ* (YJA11) strains were grown overnight at 42°C in the presence or absence of 1 M sorbitol to increase osmolarity. The fraction of lysed cells was determined by staining them with trypan blue. For comparison, cells were grown in either rich YPD medium or synthetic SD medium. The results represent the average of at least two independent experiments plus SD.

that production of Fmp45 in the absence of Sur7 may have negative effects. Altogether, these results indicate that Fmp45 does not contribute a significant function in the absence of Sur7, which is consistent with the observation that Fmp45-GFP is not stably produced in *sur7Δ* cells (Fig. 1).

## DISCUSSION

Cell wall synthesis plays a key role in *C. albicans* pathogenesis. The essential role of the cell wall for virulence is highlighted by the success of the drug caspofungin in treating infections by *C. albicans* and *A. fumigatus* (28). The cell wall also plays important roles by interacting with the immune system during infection (26). Many of the key steps of cell wall synthesis occur at the plasma membrane, where Sur7 is localized. This includes the action of  $\beta$ -glucan and chitin synthases that extrude the elongating polymers of glucose and GlcNAc, respectively, through the plasma membrane (19, 33).  $\beta$ -Glucan and chitin fibrils form the inner layer of the cell wall that gives it strength and rigidity. The outer layer is composed primarily

### A) YPD



### B) SD

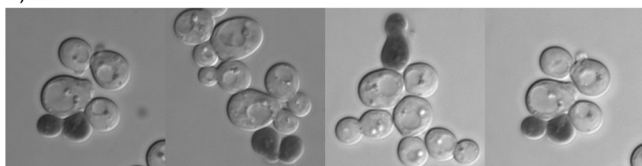


FIG. 7. Spontaneous lysis of both large and small *sur7Δ* cells. The *sur7Δ* strain YJA11 was grown at 30°C in either rich YPD (A) or synthetic SD (B) medium and then stained with trypan blue to detect lysed cells.

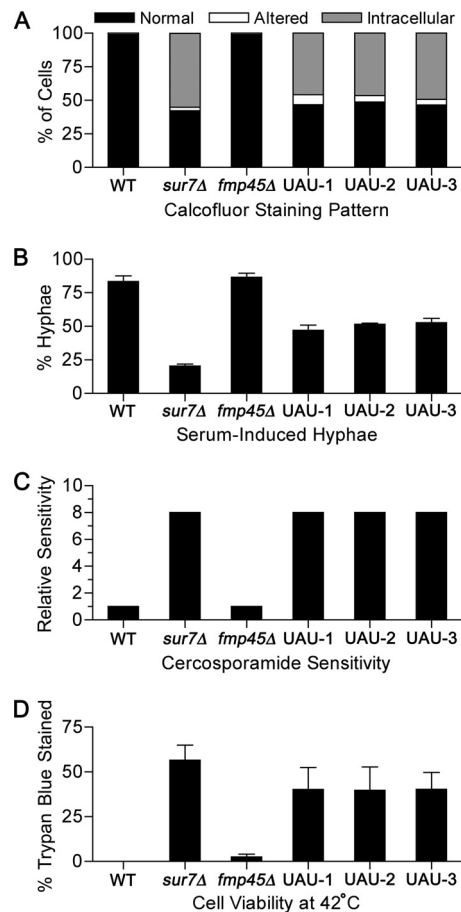


FIG. 8. Phenotypes of *sur7Δ fmp45Δ* mutants. Three *sur7Δ fmp45Δ* double mutants (UAU-1, UAU-2, and UAU-3) were generated by the UAU method as described in Materials and Methods. The mutants were compared to the following strains: wild-type control (DIC185), *sur7Δ* (YJA11), and *fmp45Δ* (YHXW3). (A) Permeabilized cells stained with calcofluor white and then examined microscopically to determine the fractions of cells displaying a normal cell wall, an altered cell wall, or an intracellular cell wall pattern ( $n = >200$ ). (B) Cells induced with 10% serum and then examined for hyphal formation ( $n = >200$ ). (C) Sensitivity to cercosporamide tested by broth dilution assays in 96-well plates. (D) Cells grown overnight at 42°C and then stained with trypan blue to determine viability ( $n = >200$ ). The error bars indicate the SD.

of different types of mannoproteins. These various cell wall components must be regulated in concert to efficiently coordinate cell wall growth.

**Cell wall function.** Previous studies demonstrated that Sur7 was needed for proper spatial regulation of cell wall growth (2). This unusual ectopic cell wall phenotype of *sur7Δ* cells also raised the question of whether the mutant cell walls could function properly. Several lines of evidence now confirm that the *sur7Δ* mutant produces defective cell walls. One is that the *sur7Δ* mutant was more sensitive to agents that exacerbate cell wall defects, including SDS, calcofluor white, and Congo red (Fig. 3) (3). However, the *sur7Δ* cells were not sensitive to all conditions that can affect cell wall mutants. For example, they were not more sensitive to elevated calcium and were only weakly sensitive to rapamycin (data not shown). Furthermore, the *sur7Δ* mutant was only slightly more sensitive to caspofun-

gin and nikkomycin Z, inhibitors of  $\beta$ -glucan and chitin synthases, respectively (Fig. 4) (2). One possible reason for the relatively small effect of caspofungin and nikkomycin Z is that the *sur7* $\Delta$  mutation might alter the coordination of cell wall synthesis but might not directly affect the enzymatic activities of the  $\beta$ -glucan and chitin synthases. Altogether, these results indicate that mutation of *SUR7* affects an important subset of cell wall functions.

As a test of cell wall strength, the *sur7* $\Delta$  mutant was examined for a cell lysis defect that could be suppressed by increased osmolarity. Growing the *sur7* $\Delta$  cells at 42°C resulted in a high proportion of lysed cells (>40%), consistent with previous observations that growth at elevated temperatures stresses the cell wall and enhances the defects of many cell wall mutants. Increasing the osmolarity of the medium by adding 1 M sorbitol partially rescued this lysis defect for the *sur7* $\Delta$  cells (Fig. 6). This confirms that the *sur7* $\Delta$  mutation causes defects in the functional properties of the cell wall, as well as in the spatial regulation of cell wall synthesis.

In contrast to Sur7, the Fmp45 protein did not have a detectable role in cell wall synthesis. The *fmp45* $\Delta$  mutant did not display altered morphogenesis or cell wall synthesis, and it was not more sensitive to a variety of conditions that were expected to exacerbate cell wall defects. Furthermore, the phenotype of a *sur7* $\Delta$  *fmp45* $\Delta$  mutant was not worse than that of the single *sur7* $\Delta$  mutant (Fig. 8). Thus, although Sur7 and Fmp45 show ~37% identity, they have distinct roles.

**Cell wall synthesis.** Chemical analysis demonstrated that the cell wall composition was significantly altered in *sur7* $\Delta$  cells (Fig. 5). In particular, the ratio of the alkali-insoluble to alkali-soluble fractions was greatly decreased, due to both a decrease in the AI fraction and an increase in the AS fraction. The increase in the AS fraction was primarily due to elevated mannan levels, which is consistent with the observation from microarray studies that the expression of the mannosyl transferase genes *MNN1* and *MNN4-4* was increased cells ~8-fold and ~5-fold, respectively, in *sur7* $\Delta$  (2). Altered mannosylation may also account for the increased sensitivity of the *sur7* $\Delta$  mutant to hygromycin, since defects in mannosylation have been linked to hypersensitivity to the drug (21). The biggest change in the AI fraction for the *sur7* $\Delta$  mutant was a decrease in  $\beta$ -glucan, the glucose polymer that constitutes the major component of the cell wall (19, 33). This decrease in  $\beta$ -glucan content is consistent with previous studies, which showed that the *sur7* $\Delta$  mutant displayed changes in gene expression and altered septin localization that were similar to effects cause by caspofungin (2, 4, 6). Furthermore, the reduced  $\beta$ -glucan levels are consistent with the formation of weaker cell walls in *sur7* $\Delta$  cells, since  $\beta$ -glucan plays a major role in cell wall strength and rigidity (22).

The next major question that needs to be resolved is whether Sur7 plays a direct or indirect role in cell wall synthesis. An indirect role is suggested by the very different patterns of subcellular localization for the static Sur7 patches and the mobile actin patches (2, 44). In *S. cerevisiae*,  $\beta$ -glucan synthase associates with mobile actin patches, which is thought to facilitate proper expansion of bud growth (11, 30, 37). In addition, Sur7-GFP is not readily detected in new buds (Fig. 1) (44), which are very active sites of cell wall synthesis. These differences in subcellular localization suggest that Sur7 is not di-

rectly involved in cell wall synthesis. However, other evidence raises the possibility that Sur7 or other MCC/eisosome proteins may directly regulate at least some aspects of cell wall synthesis. For example, an echinocandin class inhibitor of  $\beta$ -1,3-glucan synthesis was found to chemically cross-link primarily to the *C. albicans* Pil1 and Lsp1 proteins (12, 31), which are components of eisosomes that associate with Sur7 (39). In addition, a high-throughput study of *S. cerevisiae* proteins identified the Fks1 subunit of  $\beta$ -1,3-glucan synthase in a complex with Pil1 (16).

Further support for the idea that MCC/eisosomes are involved in cell wall regulation comes from analysis of the *S. cerevisiae* Pkh1/2 protein kinases, which localize to eisosomes (23, 38). In *S. cerevisiae*, Pkh1/2 regulate the Pkc1, Sch9, and Ypk1 protein kinases that act in part to control cell wall synthesis (8). Interestingly, the *C. albicans sur7* $\Delta$  cells were 8-fold more sensitive to the Pkc1 inhibitor cercosporamide (Fig. 4), similar to *C. albicans* cells with reduced Pkc1p activity (36). Since Pkc1 regulates many genes involved in cell wall synthesis, this raised the possibility that the cell wall defect of *sur7* $\Delta$  cells is due to decreased Pkc1 activity. However, other data indicate that Pkc1 is active in *sur7* $\Delta$  cells. For one, *PKC1* mutations cause the opposite effect of mutating *SUR7*. The *pkc1* mutant cells produce decreased cell wall and are not known to cause extra ectopic growth of the cell wall. Also, targets of the Pkc1-activated Rlm1 transcription factor (6) were not decreased in *sur7* $\Delta$  cells but were instead highly expressed. *PGA13* was induced 16-fold, and *CRH11* was induced 4-fold (2). Expression of cell wall synthesis genes was also not decreased in the *sur7* $\Delta$  cells. *GSCI* ( $\beta$ -1,3-glucan synthase), as well as *KRE1* and *KRE7* ( $\beta$ -1,6-glucan synthases), were expressed at slightly increased levels, and the expression of the chitin synthase genes was not changed significantly in *sur7* $\Delta$  cells (2). In contrast, there were extensive changes in the expression of genes that encode a variety of other putative cell wall proteins, especially predicted glycosylphosphatidylinositol (GPI)-anchored proteins that are likely to directly interact with the cell wall. Many of these genes are thought to be activated by the Cas5 transcription factor, which is important for response to caspofungin treatment (6). These data indicate that the cell wall defects of the *sur7* $\Delta$  cells are not due to a general failure of cells to sense and respond to cell wall damage. Future studies on MCC/eisosomes will help to define the links between these novel domains and cell wall synthesis.

#### ACKNOWLEDGMENTS

We thank the members of our laboratories for their helpful advice and comments on the manuscript, Francisco Javier Alvarez for providing strains, and Yoshikazu Ohya for advice.

This research was supported by a grant awarded to J.B.K. from the National Institutes of Health (RO1 AI47837) and a grant awarded to J.-P.L. from ERA-NET PathoGenoMics ANTIFUN.

#### REFERENCES

1. Alvarez, F. J., L. M. Douglas, and J. B. Konopka. 2009. The Sur7 protein resides in punctate membrane subdomains and mediates spatial regulation of cell wall synthesis in *Candida albicans*. *Commun. Integr. Biol.* **2**:76–77.
2. Alvarez, F. J., L. M. Douglas, A. Rosebrock, and J. B. Konopka. 2008. The Sur7 protein regulates plasma membrane organization and prevents intracellular cell wall growth in *Candida albicans*. *Mol. Biol. Cell* **19**:5214–5225.
3. Bernardo, S. M., and S. A. Lee. 2010. *Candida albicans SUR7* contributes to secretion, biofilm formation, and macrophage killing. *BMC Microbiol.* **10**: 133.



4. Blankenship, J. R., S. Fanning, J. J. Hamaker, and A. P. Mitchell. 2010. An extensive circuitry for cell wall regulation in *Candida albicans*. *PLoS Pathog.* **6**:e1000752.
5. Blankenship, J. R., and A. P. Mitchell. 2006. How to build a biofilm: a fungal perspective. *Curr. Opin. Microbiol.* **9**:588–594.
6. Bruno, V. M., et al. 2006. Control of the *C. albicans* cell wall damage response by transcriptional regulator Cas5. *PLoS Pathog.* **2**:e21.
7. Calderone, R. A., and W. A. Fonzi. 2001. Virulence factors of *Candida albicans*. *Trends Microbiol.* **9**:327–335.
8. Casamayor, A., P. D. Torrance, T. Kobayashi, J. Thorner, and D. R. Alessi. 1999. Functional counterparts of mammalian protein kinases PDK1 and SGK in budding yeast. *Curr. Biol.* **9**:186–197.
9. de Groot, P. W., et al. 2001. A genomic approach for the identification and classification of genes involved in cell wall formation and its regulation in *Saccharomyces cerevisiae*. *Comp. Funct. Genomics* **2**:124–142.
10. Dickson, R. C., C. Sumanasekera, and R. L. Lester. 2006. Functions and metabolism of sphingolipids in *Saccharomyces cerevisiae*. *Prog. Lipid Res.* **45**:447–465.
11. Drgonová, J., et al. 1996. Rho1p, a yeast protein at the interface between cell polarization and morphogenesis. *Science* **272**:277–279.
12. Edlind, T. D., and S. K. Katiyar. 2004. The echinocandin “target” identified by cross-linking is a homolog of Pil1 and Lsp1, sphingolipid-dependent regulators of cell wall integrity signaling. *Antimicrob. Agents Chemother.* **48**:4491.
13. Enloe, B., A. Diamond, and A. P. Mitchell. 2000. A single-transformation gene function test in diploid *Candida albicans*. *J. Bacteriol.* **182**:5730–5736.
14. Fontaine, T., et al. 2000. Molecular organization of the alkali-insoluble fraction of *Aspergillus fumigatus* cell wall. *J. Biol. Chem.* **275**:27594–27607.
15. Fröhlich, F., et al. 2009. A genome-wide screen for genes affecting eisosomes reveals Nce102 function in sphingolipid signaling. *J. Cell Biol.* **185**:1227–1242.
16. Gavin, A. C., et al. 2002. Functional organization of the yeast proteome by systematic analysis of protein complexes. *Nature* **415**:141–147.
17. Grossmann, G., et al. 2008. Plasma membrane microdomains regulate turnover of transport proteins in yeast. *J. Cell Biol.* **183**:1075–1088.
18. Heitman, J., S. G. Filler, J. E. J. Edwards, and A. P. Mitchell. 2006. Molecular principles of fungal pathogenesis. ASM Press, Washington, DC.
19. Klis, F. M., P. de Groot, and K. Hellingwerf. 2001. Molecular organization of the cell wall of *Candida albicans*. *Med. Mycol.* **39**(Suppl. 1):1–8.
20. Kumamoto, C. A., and M. D. Vences. 2005. Contributions of hyphae and hypha-co-regulated genes to *Candida albicans* virulence. *Cell Microbiol.* **7**:1546–1554.
21. Lambou, K., S. Perkhof, T. Fontaine, and J. P. Latge. 2010. Comparative functional analysis of the *OCH1* mannosyltransferase families in *Aspergillus fumigatus* and *Saccharomyces cerevisiae*. *Yeast* **27**:625–636.
22. Lesage, G., and H. Bussey. 2006. Cell wall assembly in *Saccharomyces cerevisiae*. *Microbiol. Mol. Biol. Rev.* **70**:317–343.
23. Luo, G., A. Gruhler, Y. Liu, O. N. Jensen, and R. C. Dickson. 2008. The sphingolipid long-chain base-Pkh1/2-Ypk1/2 signaling pathway regulates eisosome assembly and turnover. *J. Biol. Chem.* **283**:10433–10444.
24. Malinská, K., J. Malinsky, M. Opekarova, and W. Tanner. 2003. Visualization of protein compartmentation within the plasma membrane of living yeast cells. *Mol. Biol. Cell* **14**:4427–4436.
25. Malinska, K., J. Malinsky, M. Opekarova, and W. Tanner. 2004. Distribution of Can1p into stable domains reflects lateral protein segregation within the plasma membrane of living *S. cerevisiae* cells. *J. Cell Sci.* **117**:6031–6041.
26. Netea, M. G., G. D. Brown, B. J. Kullberg, and N. A. Gow. 2008. An integrated model of the recognition of *Candida albicans* by the innate immune system. *Nat. Rev. Microbiol.* **6**:67–78.
27. Odds, F. C. 1988. *Candida and candidosis*. Bailliere Tindall, Philadelphia, PA.
28. Odds, F. C., A. J. Brown, and N. A. Gow. 2003. Antifungal agents: mechanisms of action. *Trends Microbiol.* **11**:272–279.
29. Pringle, J. R. 1991. Staining of bud scars and other cell wall chitin with calcofluor. *Methods Enzymol.* **194**:732–735.
30. Qadota, H., et al. 1996. Identification of yeast Rho1p GTPase as a regulatory subunit of 1,3-beta-glucan synthase. *Science* **272**:279–281.
31. Radding, J. A., S. A. Heidler, and W. W. Turner. 1998. Photoaffinity analog of the semisynthetic echinocandin LY303366: identification of echinocandin targets in *Candida albicans*. *Antimicrob. Agents Chemother.* **42**:1187–1194.
32. Reuss, O., A. Vik, R. Kolter, and J. Morschhauser. 2004. The *SATI* flipper, an optimized tool for gene disruption in *Candida albicans*. *Gene* **341**:119–127.
33. Ruiz-Herrera, J., M. V. Elorza, E. Valentin, and R. Sentandreu. 2006. Molecular organization of the cell wall of *Candida albicans* and its relation to pathogenicity. *FEMS Yeast Res.* **6**:14–29.
34. Sherman, F. 1991. Getting started with yeast. *Methods Enzymol.* **194**:3–21.
35. Sudbery, P., N. Gow, and J. Berman. 2004. The distinct morphogenic states of *Candida albicans*. *Trends Microbiol.* **12**:317–324.
36. Sussman, A., et al. 2004. Discovery of cercosporamide, a known antifungal natural product, as a selective Pkc1 kinase inhibitor through high-throughput screening. *Eukaryot. Cell* **3**:932–943.
37. Utsugi, T., et al. 2002. Movement of yeast 1,3-beta-glucan synthase is essential for uniform cell wall synthesis. *Genes Cells* **7**:1–9.
38. Walther, T. C., et al. 2007. Pkh-kinases control eisosome assembly and organization. *EMBO J.* **26**:4946–4955.
39. Walther, T. C., et al. 2006. Eisosomes mark static sites of endocytosis. *Nature* **439**:998–1003.
40. Whiteway, M., and U. Oberholzer. 2004. *Candida* morphogenesis and host-pathogen interactions. *Curr. Opin. Microbiol.* **7**:350–357.
41. Wilson, R. B., D. Davis, and A. P. Mitchell. 1999. Rapid hypothesis testing with *Candida albicans* through gene disruption with short homology regions. *J. Bacteriol.* **181**:1868–1874.
42. Xu, D., et al. 2007. Genome-wide fitness test and mechanism-of-action studies of inhibitory compounds in *Candida albicans*. *PLoS Pathog.* **3**:e92.
43. Xu, T., et al. 2010. A profile of differentially abundant proteins at the yeast cell periphery during pseudohyphal growth. *J. Biol. Chem.* **285**:15476–15488.
44. Young, M. E., et al. 2002. The Sur7p family defines novel cortical domains in *Saccharomyces cerevisiae*, affects sphingolipid metabolism, and is involved in sporulation. *Mol. Cell. Biol.* **22**:927–934.
45. Zhang, C., and J. B. Konopka. 2010. A photostable green fluorescent protein variant for analysis of protein localization in *Candida albicans*. *Eukaryot. Cell* **9**:224–226.